Journal of Energy Chemistry 30 (2019) 108–113

Contents lists available at ScienceDirect

Journal of Energy Chemistry

journal homepage: www.elsevier.com/locate/jechem

http://www.journals.elsevier.com/journal-of-energy-chemistry/

First-principles kinetics study of carbon monoxide promoted Ostwald ripening of Au particles on FeO/Pt(111)

Sulei Hu[a,d,1], Runhai Ouyang[a,d,1], Wei-Xue Li[a,b,c,*]

[a] State Key Laboratory of Catalysis, Dalian Institute of Chemical Physics, Chinese Academy of Sciences, Dalian 116023, Liaoning, China
[b] Department of Chemical Physics, School of Chemistry and Materials Science, iCHeM, CAS Excellence Center for Nanoscience, University of Science and Technology of China, Hefei 230026, Anhui, China
[c] Hefei National Laboratory for Physical Sciences at the Microscale, Hefei 230026, Anhui, China
[d] University of Chinese Academy of Sciences, Beijing 100049, China

ARTICLE INFO

Article history:
Received 8 February 2018
Revised 12 March 2018
Accepted 21 March 2018
Available online 10 April 2018

Keywords:
Carbon monoxide
Au particles
Ostwald ripening
First-principles kinetics
FeO/Pt(111)

ABSTRACT

The dynamic and kinetic evolution of supported metal particles in the presence of reactants is decisive in shaping the nature of the catalytic active sites and the deactivation process. Ostwald ripening of FeO/Pt(111) supported Au particles in the presence of carbon monoxide is addressed here by first-principles kinetics. It is found that CO stabilizes the ripening monomer (Au atom) by forming favorable Au carbonyls with lower total activation energy, and corresponding phase diagram at wide range of temperature and CO pressures is constructed. Evolution of particle number, dispersion and particle size distribution of supported Au particles are explored. Great influence of CO promotion on ripening kinetics is revealed and explored in details, and mbar range of CO can lower the onset temperature of ripening by a few hundred kelvins. The present work reveals the crucial role of the metal-reactant complexes formed under reaction conditions on ripening of metal catalysts.

1. Introduction

The dynamic and kinetic evolution of supported metal particles under reaction conditions [1–3] is decisive in shaping the nature of the catalytic active sites and the deactivation process [4,5]. Under reaction conditions, the adsorption of reactants on supported particles can lower the surface energy, influence the corresponding morphology [6–8] and even cause the wetting of metal particles on the supports [9,10]. In particular, adsorption of reactants on particles could weaken the metal-metal bonding of supported particles [11], and facilitate the detachment/attachment of the metal monomer from/towards the particles, and stabilize the detached metal monomer by forming the metal-reactant complexes on the supports [12,13]. The presence of reactants may lead to the deactivation of supported particles because of promoted ripening via mass transport on the surface [14–24] or due to volatile loss [25]. In extreme conditions, strong metal-reactant interaction could even break up the stepped surfaces [26,27] and completely disintegrate the supported precious metal particles, for example, rhodium [28–30]. Dramatic changes of catalyst structures at elevated temperature and pressure, having profound influence on the corresponding catalytic activity and stability, causes the so-called pressure gap, which necessitates the mechanistic understanding of how reactants cause the changes and how can we control or prevent the changes.

Gold particles supported on oxide surfaces with unique size-dependent catalytic selectivity and low temperature activity [31,32] are among the notable examples manifesting the influence of reaction conditions [33–35]. In ultrahigh vacuum, supported Au particles were stable up to annealing temperature of 600 K [36]. In the presence of reactant, it was reported that chlorides can promote the ripening of supported Au particles [37,38]. In the presence of CO oxidation atmosphere, the ripening temperature of Au particles shifts to a much lower temperature (430 K) [39–42]. Recent ab initio molecular dynamics studies showed that the Au-carbonyl complexes can be formed dynamically in CO oxidation reaction [43,44]. Also, the thermal resistance of metal particles can be reduced because of the formation of volatile metal-chloride, metal-oxygen [45] or metal-carbonyl [46–53] complexes. Formation of the metal-reactant complexes was believed to promote the Ostwald ripening, facilitating the growth of larger ones at the expense of smaller ones, resulting in eventually catalyst deactivation [54–59].

* Corresponding author at: State Key Laboratory of Catalysis, Dalian Institute of Chemical Physics, Chinese Academy of Sciences, Dalian 116023, Liaoning, China.
E-mail address: wxli70@ustc.edu.cn (W.-X. Li).
[1] These authors contributed equally to this work.

https://doi.org/10.1016/j.jechem.2018.03.023

Despite the extensive studies so far [60,61], microscopic understanding for the role of the Au carbonyl complexes on the ripening is still not well understood. A particularly interesting system is the Au particles supported on FeO/Pt(111) in the presence of CO reactant [62,63]. It was found that small Au particles decorated at the step edges were very stable under pure O_2 environment at room temperature (RT), but they disappeared gradually under 1 mbar pure CO. The disintegrated small Au particles were believed to form mobile Au species that migrate across the FeO film surface [64]. Clearly the reactant CO destabilized the supported Au particles. However, it is unclear yet when the Au carbonyl will form and how temperature and CO partial pressure will influence the ripening kinetics of Au particles on FeO/Pt(111). To address these questions, detailed energetic and kinetic investigations taking account of the influence of temperature and pressure are required.

Stability of supported metal catalysts under reaction conditions has been studied extensively by density function theory (DFT) [65,66] and molecular dynamics [67]. However, a systematic ripening kinetics study based on first-principles calculation for supported Au particles in the presence of CO has not been reported yet. In this work, we carried out Ostwald ripening kinetic investigations of Au particles supported on FeO/Pt(111) in the presence of CO, taking account of the influence of temperature and pressure. Employing the atomistic Ostwald ripening (OR) theory in the presence of reactant [68] and DFT calculations, we confirmed the ripening of supported Au particles on FeO/Pt(111) in presence of CO, and clarified the critical roles of reactant on the ripening. In Section 2, we describe the reactant assisted Ostwald ripening theory and DFT calculation details. In Section 3, we first present the energetics from DFT calculations, and then we show the changes of total activation energy of OR against the CO chemical potential and the corresponding phase diagrams with respect to CO pressure and temperature, followed by OR kinetic simulation results. Final conclusions are made in Section 4.

2. Theory and method

For supported metal particles in the presence of reactants, the reactants could adsorb on both the metal particle and the metal atoms in thermodynamic equilibrium with the particles under the "steady-state" [60,61]. For a particle on support with a given curvature radius R, the corresponding ripening kinetic rate equation under the mean field approximation is [68]

$$\frac{dR}{dt} = \frac{XY}{X+Y}\frac{K}{R^2}\left(\exp\left[-\frac{E^{tot}}{kT}\right]\right) \times \left(\exp\left[\frac{\Delta\mu_{NP}(R^*)}{kT}\right] - \exp\left[\frac{\Delta\mu_{NP}(R)}{kT}\right]\right) \quad (1)$$

where $K = \nu_s\Omega/[4\pi a_0{}^2\alpha_1]$ with $\alpha_1 = [2\text{–}3\ \cos(\alpha) + \cos^3(\alpha)]/4$; α is the contact angle between the metal particles and the support as a measurement of metal particle-support interaction; ν_s is the vibration frequency of monomer species on supports, which will be considered as constant $6 \times 10^{13}\ s^{-1}$ as a good approximation [69–72]; Ω is the volume of bulk metal atoms (16.96 Å^3 for Au) [73]; a_0 is the lattice constant of the support (3.10 Å for FeO/Pt(111)) [62,63]. $X = 2\pi a_0 R\sin(\alpha)$, $Y = 2\pi a_0{}^2/\ln[L/(R\ \sin\alpha)]$ with L being the diffusion length representing the distance required for the concentration of monomer species reaching the far field critical value. In this work, L was set to $1.2R\sin\alpha$ [74].

$\Delta\mu_{NP}$ is the chemical potential of metal atoms in the supported metal particle with respect to that of infinite size (bulk) in the presence of reactants, and is approximated here by the Gibbs-Thomson (GT) relation, [68]

$$\Delta\mu_{NP}(R) = \frac{2\Omega\gamma}{R} \quad (2)$$

where γ is the surface energy of the particle of interest. When particle size is small (for instance less than 5 nm), γ might become size dependent due to the decreasing of the coordination number of surface atoms as the size decreases. The size-dependence of γ will be ignored for simplicity considering modest influencing on the conclusions in next section [60], and surface energy of 0.94 eV/Å^2 [75] is used in this work. Note that under a given particle (constant particle volume V_p), the different metal support interactions (therefore different α) would lead to different curvature radius based on $R = (3V_p/4/\alpha_1)^{1/3}$, accordingly the influence of the metal-support interaction is included implicitly in GT equation. Recently, the GT-like relation explicitly taking into account the effect of supports was addressed recently [76,77].

The total activation energy E^{tot} of the ripening is decisive to the ripening rate [68]. In the presence of reactant CO, both the Au atoms and the as formed Au carbonyls could contribute to the ripening process. The E^{tot} via the route with monomer to be Au atoms or Au carbonyls are

$$E^{tot}_{at} = E^{f}_{at} + E^{d}_{at} \quad (3)$$

$$E^{tot}_{carb} = E^{f}_{carb} + E^{d}_{carb} - n\ \times\ \Delta\mu_{CO}(T,P) \quad (4)$$

respectively. E^{d}_{at} and E^{d}_{carb} are the diffusion barriers of the metal atoms and the metal carbonyls on supports, and n is the number of CO in the carbonyls. E^{f}_{at} is the formation energy of the metal atoms with respect to bulk counterpart. E^{f}_{carb} is the formation energy of the metal carbonyls with respect to bulk Au and gas phase CO.

$\Delta\mu_{CO}$ is CO chemical potential, a function of temperature and CO partial pressure, $\Delta\mu_{CO}(T,P) = \Delta\mu^{\circ}_{CO}(T,P^{\circ}) + kT\ln(P/P^{\circ})$, where k is the Boltzmann constant, and $\Delta\mu^{\circ}_{CO}(T,P^{o})$ is the chemical potential of CO at standard conditions P° [78]. The active intermediates for ripening are Au atoms if $E^{tot}_{at} < E^{tot}_{carb}$, but the Au carbonyl if $E^{tot}_{carb} < E^{tot}_{at}$. To have $E^{tot}_{carb} \le E^{tot}_{at}$, the corresponding $\Delta\mu_{CO}$ must satisfy:

$$\Delta\mu_{CO} \ge \left(E^{f}_{carb} + E^{d}_{carb} - E^{f}_{at} - E^{d}_{at}\right)/n \quad (5)$$

From Eq. (4), we see the total activation energy of reactant assisted OR is contributed by the carbonyls formation energy and their diffusion barrier on the support of interest, and also the chemical potential of the reactants. All these quantities will be carefully discussed later. When the diffusion barrier is larger than the formation energy, the ripening kinetics is noted as diffusion control, and interface control otherwise [60,61]. The presence of reactants could stabilize the metal atoms, changing the OR monomer from metal atoms to metal carbonyls. As a result, the rate-determining step (diffusion control or interface control) of reactant assisted ripening kinetics could be quite different from that without reactants.

Particle size distribution (PSD) of supported particles is assumed here to follow a Gaussian distribution $f(R, t)$ with average size $< R >$ and standard deviation σ. The mass conservation gives

$$\frac{4}{3}\pi\alpha_1\int_0^{\infty} f(R,t)R^3 dR = V_0 \quad (6)$$

where V_0 is the initial total volume of supported metal particles. The particle number $N(t)$ evolves with time as below

$$N(t) = \int_0^{\infty} f(R,t)dR \quad (7)$$

Ripening kinetics under isothermal and temperature programed aging (TPA) condition were considered, and corresponding dispersion, particle number and average size are calculated. For TPA, the initial temperature is 300 K, and the temperature ramping rate is 1 K/s.

Spin-polarized DFT calculations were performed, using the code Vienna Ab Initio Simulation Package (VASP) [79], to obtain

the energetics as input for the OR simulation. The core-valence electron interaction was described by the projector augmented wave (PAW). [80] The exchange-correlation was described by the Perdew-Wang functional [81] within the generalized-gradient approximation (GGA). For the superstructure model of FeO/Pt(111) (see below), the cutoff energy for expanding the wave function using plane waves was set to 350 eV with which the energetics already converge to the accuracy request for Au adsorption [63]. Diffusion barriers of Au atoms and Au-CO monomers on the supports of FeO/Pt(111) were calculated using the climbing image nudged elastic band (CI-NEB) method [82]. The FeO/Pt(111) was simulated by the slab model: $(\sqrt{84}\times\sqrt{84})$ $R10.9°$, where the FeO(111) bilayer is supported on a three-layer-Pt [62,63]; Only gamma k-point was used for the Brillouin zone. Structure relaxations were performed using the conjugate-gradient algorithm and stopped when the force components on each atom are less than 0.03 eV/Å. The bottom two layers of Pt in FeO/Pt(111) were fixed to their bulk positions during structure relaxations. In addition, the DFT + U corrections were considered for the iron atoms in FeO/Pt(111), with $U_{\mathrm{eff}}(U-J)=3.0$ eV [63].

3. Results and discussion

3.1. Energetics from DFT

The formation energy and diffusion barrier of the Au atoms and carbonyls are the key quantities determining the rate of ripening, and they form an important basis for further thermodynamic analysis and kinetic evolution. The calculated most stable adsorption configurations of Au atom and Au-CO on FeO/Pt(111) surface are shown in Fig. 1(a, b), and favored diffusion paths are shown in Fig. 1(c). On FeO/Pt(111), there are FCC, HCP and top three domains in the Moiré supercell [62,63]. The most stable adsorption site of the Au atom was found at the Fe-top in the HCP domain, as shown in Fig. 1(a), with the formation energy $E^{\mathrm{f}}_{\mathrm{at}}=2.03$ eV. The most stable adsorption in the other two domains also take the Fe-top sites, but is 0.11 eV and 0.07 eV less stable in FCC and Top domains, respectively, than that in HCP domain. The strong preference of Au on Fe-top over O-top site comes mainly from the pronounced electrostatic attraction between anionic Au and cationic Fe. Formation of anionic Au is likely since Au has a rather high electronegativity thank for its significant relativistic effects [63]. The favored diffuse path of Au atom was found from one Fe-top to another Fe-top site, as indicated by the blue arrow in Fig. 1(c), with a barrier of 0.39 eV. Since the formation energy is considerably larger than the diffusion barrier, corresponding ripening process is interface control. The resulted total activation energy is 2.42 eV, and the large value indicates that in absence of reactant, Au particles supported on FeO/Pt(111) have high ripening resistance.

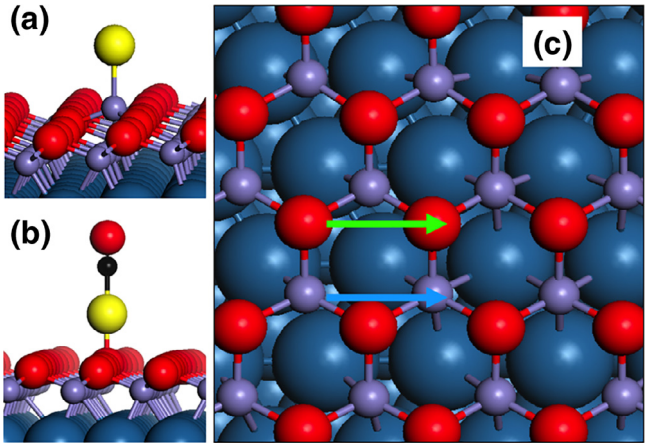

Fig. 1. The most stable adsorption sites of the Au atom at Fe-top site (a) and Au-CO carbonyl at O-top site (b) on the oxide surfaces. (c) Diffusion pathways of Au atom (blue arrow) and Au carbonyl (green arrow) on FeO/Pt(111) in top view. Color code: yellow: Au; red, O; black, C; blue: Fe; dark cyan, Pt. (For interpretation of the references to color in this figure legend, the reader is referred to the web version of this article.)

For Au carbonyls, both the adsorption of Au-CO and Au-$(CO)_2$ were calculated, and it was found that the Au-$(CO)_2$ on FeO/Pt(111) was unstable and therefore neglected in following discussion. We tested adsorption of Au-CO at O-top, O-fcc, and O-hcp in each of the three domains. The most stable adsorption site was found at the O-top in the FCC domains, as shown in Fig. 1(b), and corresponding diffusion path is shown in Fig. 1(c). The calculated formation energy of Au-CO $E^{\mathrm{f}}_{\mathrm{carb}}$ is −0.07 eV in FCC domain (0.06 eV in HCP and 0.46 eV in Top domain, both also at O-top sites), and the barrier for Au-CO diffusion between two O-top sites $E^{\mathrm{d}}_{\mathrm{carb}}$ is 0.48 eV. This shows clearly that the CO adsorption on the Au atoms dramatically lowers the formation energy of the intermediates for the ripening. Corresponding total activation energy under CO rich condition ($\Delta\mu_{\mathrm{CO}}=0$ eV) becomes 0.41 eV only, which is significantly lower than that of Au atom. It can be expected that the presence of CO would promote ripening of supported Au particles, which will be discussed in detail below. The site preference of Au-CO over O-top comes from the formation of cationic Au, which would maximize the donation and back-donation between CO and Au.

The stabilization of Au atom by CO can be justified by the strong binding between CO and Au atom on FeO/Pt(111). DFT calculations show the binding energy of CO with the Au atom is −2.55 eV. Also, we found the Bader charge of the Au of the carbonyls on the polar FeO/Pt(111) [62,63] is +0.72 |e|. As a result, CO form strong bond with the Au cation, which is mainly due to electrostatic interaction between the CO dipole and the positive charge of Au cation [83].

3.2. Total activation energies

As indicated in Eqs. (3) and (4), the total activation energy for Au carbonyl is dependent on CO chemical potential. When CO chemical potential is low ($\Delta\mu_{\mathrm{CO}}<E^{\mathrm{b}}_{\mathrm{CO}}$), the energy gain from CO binding towards Au atom ($E^{\mathrm{b}}_{\mathrm{CO}}$) cannot compensate the loss of CO entropy in gas phase, and then the formation of Au carbonyls is unlikely. When $\Delta\mu_{\mathrm{CO}}\geq E^{\mathrm{b}}_{\mathrm{CO}}$, CO can adsorb on top of the Au atoms, and the Au carbonyls start to form. When $\Delta\mu_{\mathrm{CO}}$ increases to such a value defined in Eq. (5), $E^{\mathrm{tot}}_{\mathrm{carb}}\leq E^{\mathrm{tot}}_{\mathrm{at}}$, the Au carbonyls become the dominating intermediates for ripening.

Fig. 2(a) shows the total activation energies versus CO chemical potential. At low $\Delta\mu_{\mathrm{CO}}$, Au atom are the dominating species for ripening, with a large total activation energy of 2.42 eV, and corresponding mechanism is interface control. The threshold $\Delta\mu_{\mathrm{CO}}$ for Au-CO carbonyl to become the dominating ripening intermediate ($\bar{E}^{\mathrm{tot}}_{\mathrm{carb}}<\bar{E}^{\mathrm{tot}}_{\mathrm{at}}$) is −2.01 eV on FeO/Pt(111). After the threshold, the total activation energy decreases linearly with CO chemical potential. The mechanism changes from interface control to diffusion control when the $\Delta\mu_{\mathrm{CO}}$ increase up to −0.55 eV. Under CO rich condition ($\Delta\mu_{\mathrm{CO}}=0$ eV), the corresponding value becomes 0.41 eV.

Contour plot of the total activation energy with respect to temperature and CO partial pressure P_{CO} is plotted in Fig. 2(b). It can be found that with increase of P_{CO} (equivalent to increase CO chemical potential), the corresponding total activation energy decreases. Namely, raising P_{CO} can lower considerably the total activation energy. Whereas with increase of temperature (equivalent to decrease CO chemical potential), the corresponding total activation energy increases. Actually, when temperature is sufficiently high, Au carbonyl could decompose, and the Au atom becomes

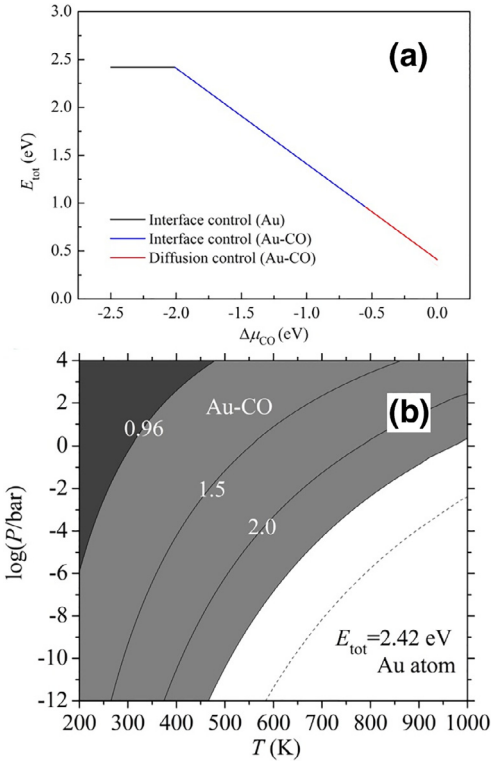

Fig. 2. (a) The total activation energies of Au OR on FeO/Pt(111) versus the CO chemical potential. (b) Contour plot of the total activation energy of Au OR on FeO/Pt(111) as functions of temperature and logarithm of CO partial pressure. The white area indicates the active ripening species is Au atoms, with a constant total activation energy and the mechanism of interface control. The dashed-line indicates the onset of formation of the Au carbonyls. The grey and dark areas indicate the active ripening species are the Au carbonyls, with the mechanism changing from interface control in the grey area to diffusion control in the dark grey area.

the dominating ripening intermediate again. It can be found from Fig. 2(b) that the same total activation energy can be reached by different combinations of T and P_{CO}, with the same CO chemical potential. Nevertheless, even though their total activation energy is the same, corresponding kinetics are different because of their different temperatures.

3.3. Ostwald ripening of Au@FeO/Pt(111) in the presence of CO

Kinetic simulation of the Au particle ripening in the presence of CO was performed to see the influence of ambient condition on FeO/Pt(111). Particle size distribution (PSD) for supported Au particles was assuming to follow a Gaussian distribution with the average particle size $< d > = 2.5$ nm and standard deviation $\sigma = 0.3$ nm (Fig. 3) throughout the present work unless stated otherwise. Calculated contact angle of Au particle on perfect FeO/Pt(111) surface is 43.6°, based on the height/diameter ratio ~0.2 of Au supported on FeO/Pt(111) reported in Ref. [84].

We first studied the ripening of Au particles without CO adsorption under temperature programing condition with heating rate 1 K/s. In this process, the total activation energy is constant ($E_{at}^{tot} = 2.42$ eV). Fig. 4(a) shows the evolution of the normalized total volume V, the particle number N and dispersion D (the ratio between number of surface and bulk atom number) with respect to the ramping temperature starting from 300 K. No changes for both D and N can be observed before the temperature of 700 K. At 750 K, the N and D decrease about 10% and 13%, respectively. To characterize the thermal resistance and simplify the analysis below, we define the temperature for 10% decrease of the particle number as onset temperature T_{on}. After this temperature, both N

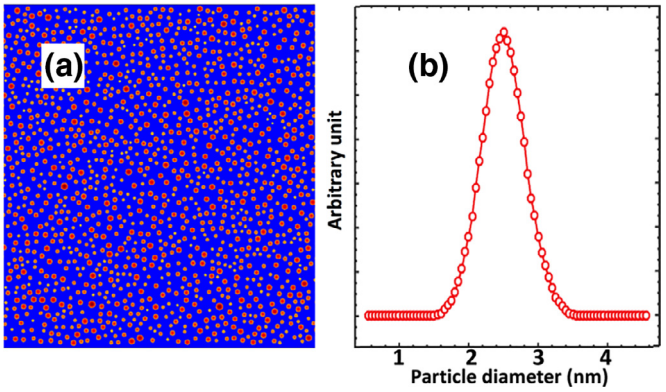

Fig. 3. (a) Schematic of supported Au particles; and (b) the corresponding particle size distribution. Contact angle $\alpha = 43.6°$; average diameter $< d > = 2.5$ nm; standard deviation $\sigma = 0.3$ nm.

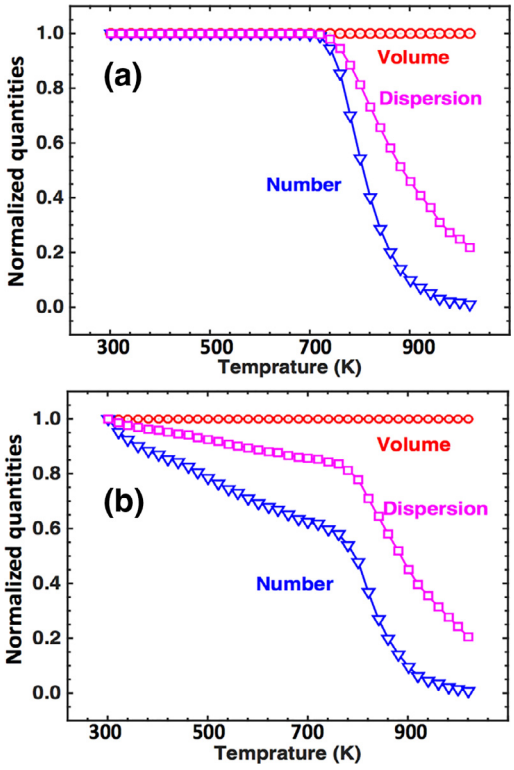

Fig. 4. (a) Evolution of normalized particle number, dispersion and volume with temperature without the presence of CO; and (b) with the presence of 1 mbar CO for FeO/Pt(111) supported Au particles in a linear temperature ramp at a rate of 1 K/s from 300 K to 1023 K.

and D drops rapidly, and at temperature 950 K, all the initial small particles ripen into a few large particles, as indicated in PSD (Figs. 4a and 5a). Throughout the whole ripening process, the total volume V is constant, indicating the mass conservation during simulation.

At elevated pressure, CO could adsorb and stabilize Au atom by forming Au carbonyls. To see this, the ripening under 1 mbar CO was investigated. Different from the results without CO, both D and N start to decrease at the very beginning of ramping process (300 K, Fig. 4b), and decreases linearly with ramping temperature. Corresponding T_{on} becomes 480 K. Dramatic influence can also be seen from the rapid evolution of PSD (Fig. 5b). As aforementioned, the total activation energy increase with ramping temperature because of decrease in CO chemical potential. Thus, the

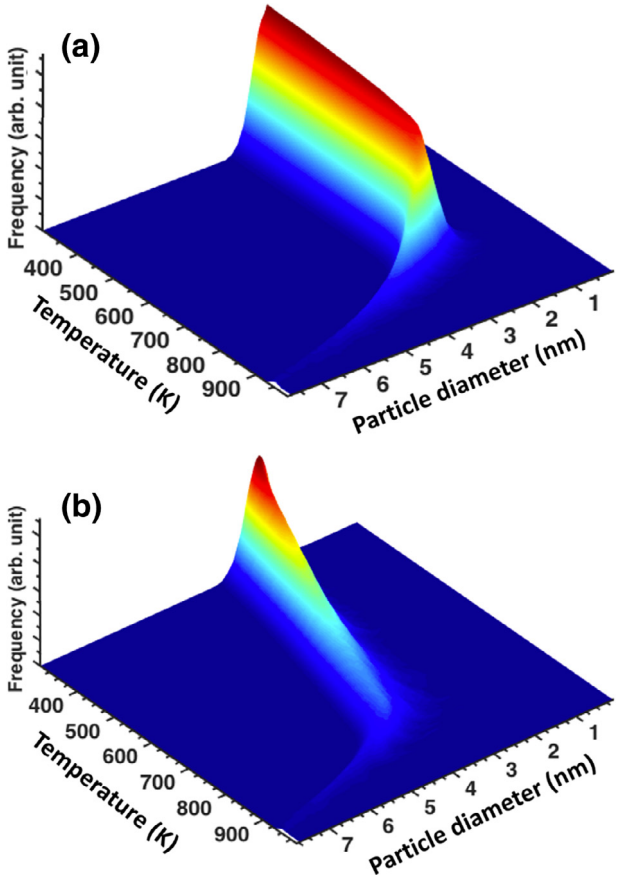

Fig. 5. Evolution of the three-dimensional particle size distribution for FeO/Pt(111) supported Au particles with a linear temperature ramping from 300 K without the presence of CO (a) and with the presence of 1 mbar CO (b).

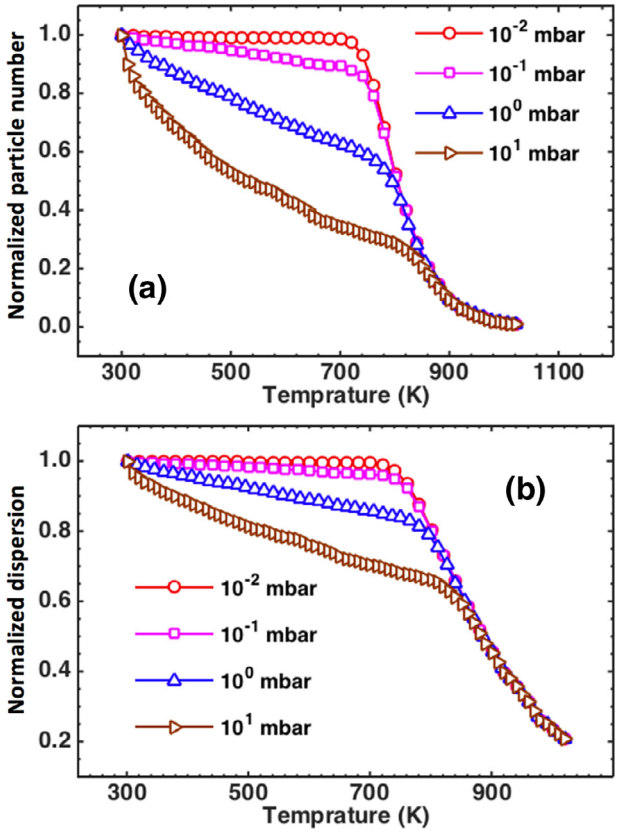

Fig. 6. Evolution of normalized particle number (a) and dispersion (b) versus ramping temperature for FeO/Pt(111) supported Au particles under CO partial pressure of 0.01, 0.1, 1 and 10 mbar.

role of promotion of CO via carbonyls on ripening will be reduced at high temperature. Eventually, formation of Au carbonyl will be no longer favorable, and the Au atoms become the dominating ripening intermediates again. Fig. 4(b) clearly shows such turning point at 770 K. Further increase of ramping temperature drive both N and D drop steeply (Fig. 4b).

Fig. 6(a, b) shows the evolution of N and D versus ramping temperature process under different CO partial pressures, respectively. For $P_{CO} = 0.01$, 0.1 and 1 mbar, corresponding total activation energies E^{tot}_{carb} are 1.24, 1.18, and 1.12 eV at 300 K. The higher the CO pressure, the smaller the total activation energy E^{tot}_{carb}, and the faster the ripening rate. Indeed, Fig. 6(a, b) shows that at a temperature in range from 300 K to 700 K, the higher the CO pressure, the lower the particle number and dispersion. As a result, corresponding T_{on} decrease from 750 K to 680 K, 400 K, and 310 K, for the CO pressure of 0.01, 0.1, 1, and 10 mbar, respectively. Consistent with the lower T_{on} at higher P_{CO}, the Au carbonyl as ripening intermediate is more stable and tolerant of higher ramping temperature.

As a comparison, T_{on} in absence of CO was also calculated, and the corresponding result is 750 K. When P_{CO} applied is low (0.01 mbar), CO cannot adsorb on Au adatom, and the calculated T_{on} (750 K) remains the same with that without the presence of CO. When $\Delta\mu_{CO} \geq -2.01$eV ($P_{CO} \geq 10^{-1.25}$ mbar when $T = 750$ K), $E^{tot}_{carb} \leq E^{tot}_{at}$, and the Au carbonyls become dominating intermediate for the ripening. This is indeed found from the apparent decline for 0.1 mbar in our kinetics simulation (Fig. 6a). The results tell that CO promotion for FeO/Pt(111) supported Au particles of ~2.5 nm happens at 0.1 mbar.

To rationalize this, we note that without CO, T_{on} on FeO/Pt(111) has a relative high value 750 K, with a large E^{tot}_{at}. When $\Delta\mu_{CO} \geq -2.01$ eV at $T = 750$ K, CO partial pressure of 0.1 mbar is already sufficient for promoting ripening. With further increase of CO partial pressure, onset temperature decreases dramatically. Great influence of CO on FeO/Pt(111) supported Au particles was observed by scan tunnelling microscope (STM) [64]. Instead of CO promotion on the ripening, it was found that when CO partial pressure was about 2 mbar at RT, Au particles decorated at FeO/Pt(111) edges disappeared, and a mobile species "invisible" in the STM images is proposed to form on the support surface. Actually, our calculations using the disintegration theory [68] show that at this pressure, the disintegration of the Au particles into the Au carbonyls is thermodynamically more favorable. Calculated low diffusion barrier (0.48 eV) of the Au carbonyl on FeO/Pt(111) also explains why the disintegrated Au carbonyls would be hardly observed by STM operated at RT.

4. Conclusions

Ostwald ripening of Au particles on the surfaces of FeO/Pt(111) with and without the presence of carbon monoxide are studied by first-principles thermodynamics and kinetics simulation. Great CO promotion on ripening of Au particles on FeO/Pt(111) surface is identified, and influence of the reactants on ripening kinetics at wide range of temperature and CO partial pressure is quantified. Without the presence of CO, calculated total activation energies of the Au atom as the active species for ripening are considerably large, and the ripening process is interface control. The presence of reactants can stabilize the metal atoms forming favorable metal-reactant complexes, lower the total activation energies

of ripening, promoting significantly the ripening kinetics of supported metal particles. It is found that the CO can lower the onset temperature of ripening by more than 300 K at CO partial pressure of 1 mbar. This work provides insights into the importance of ambient conditions on Ostwald ripening of supported metal particles, and the role of the reactant-metal complexes formed under reaction conditions in facilitation on ripening is highlighted.

Acknowledgments

This work was supported by the National Key R&D Program of China (2017YB0602205), the National Natural Science Foundation of China (91645202), and the Chinese Academy of Sciences (QYZDJ-SSW-SLH054).

Reference

[1] F. Tao, M. Salmeron, Science 331 (2011) 171–174.
[2] F. Tao, P.A. Crozier, Chem. Rev. 116 (2016) 3487–3539.
[3] J. Dou, Z.C. Sun, A.A. Opalade, N. Wang, W.S. Fu, F. Tao, Chem. Soc. Rev. 46 (2017) 2001–2027.
[4] C.H. Bartholomew, Appl. Catal. A 212 (2001) 17–60.
[5] J.A. Moulijn, A.E. van Diepen, F. Kapteijn, Appl. Catal. A 212 (2001) 3–16.
[6] T. Uchiyama, H. Yoshida, Y. Kuwauchi, S. Ichikawa, S. Shimada, M. Haruta, S. Takeda, Angew. Chem. Int. Ed. 50 (2011) 10157–10160.
[7] P. Nolte, A. Stierle, N.Y. Jin-Phillipp, N. Kasper, T.U. Schulli, H. Dosch, Science 321 (2008) 1654–1658.
[8] P.L. Hansen, J.B. Wagner, S. Helveg, J.R. Rostrup-Nielsen, B.S. Clausen, H. Topsoe, Science 295 (2002) 2053–2055.
[9] K.H. Ernst, A. Ludviksson, R. Zhang, J. Yoshihara, C.T. Campbell, Phys. Rev. B 47 (1993) 13782–13796.
[10] C.T. Campbell, Surf. Sci. Rep. 27 (1997) 1–111.
[11] A. Kolmakov, D.W. Goodman, Catal. Lett. 70 (2000) 93–97.
[12] Z. Łodziana, J.K. Nørskov, J. Chem. Phys. 115 (2001) 11261–11267.
[13] R. Meyer, J. Lockemeyer, R. Yeates, M. Lemanski, D. Reinalda, M. Neurock, Chem. Phys. Lett. 449 (2007) 155–159.
[14] M.A. Newton, Chem. Soc. Rev. 37 (2008) 2644–2657.
[15] S.B. Simonsen, I. Chorkendorff, S. Dahl, M. Skoglundh, J. Sehested, S. Helveg, J. Am. Chem. Soc. 132 (2010) 7968–7975.
[16] T.W. Hansen, A.T. Delariva, S.R. Challa, A.K. Datye, Acc. Chem. Res. 46 (2013) 1720–1730.
[17] C.G. Granqvist, R.A. Buhrman, J. Catal. 42 (1976) 477–479.
[18] F. Behafarid, B. Roldan Cuenya, Surf. Sci. 606 (2012) 908–918.
[19] S.R. Challa, A.T. Delariva, T.W. Hansen, S. Helveg, J. Sehested, P.L. Hansen, F. Garzon, A.K. Datye, J. Am. Chem. Soc. 133 (2011) 20672–20675.
[20] J. Sehested, J.A.P. Gelten, S. Helveg, Appl. Catal. A 309 (2006) 237–246.
[21] J. Sehested, N.W. Larsen, H. Falsig, B. Hinnemann, Catal. Today 228 (2014) 22–31.
[22] M. Sadeqzadeh, J.P. Hong, P. Fongarland, D. Curulla-Ferre, F. Luck, J. Bousquet, D. Schweich, A.Y. Khodakov, Ind. Eng. Chem. Res. 51 (2012) 11955–11964.
[23] T.O. Eschemann, K.P. de Jong, ACS Catal. 5 (2015) 3181–3188.
[24] D. Kistamurthy, A.M. Saib, D.J. Moodley, J.W. Niemantsverdriet, C.J. Weststrate, J. Catal. 328 (2015) 123–129.
[25] P.J.F. Harris, Int. Mater. Rev. 40 (1995) 97–115.
[26] F. Tao, S. Dag, L.-W. Wang, Z. Liu, D.R. Butcher, H. Bluhm, M. Salmeron, G.A. Somorjai, Science 327 (2010) 850–853.
[27] S. Horch, H.T. Lorensen, S. Helveg, E. Laegsgaard, I. Stensgaard, K.W. Jacobsen, J.K. Norskov, F. Besenbacher, Nature 398 (1999) 134–136.
[28] A. Berko, F. Solymosi, J. Catal. 183 (1999) 91–101.
[29] A. Suzuki, Y. Inada, A. Yamaguchi, T. Chihara, M. Yuasa, M. Nomura, Y. Iwasawa, Angew. Chem. Int. Ed. 42 (2003) 4795–4799.
[30] S.M. McClure, M.J. Lundwall, D.W. Goodman, Proc. Natl. Acad. Sci. USA. 108 (2011) 931–936.
[31] E. Roduner, Chem. Soc. Rev. 35 (2006) 583–592.
[32] B. Hvolbaek, T.V.W. Janssens, B.S. Clausen, H. Falsig, C.H. Christensen, J.K. Norskov, Nano Today 2 (2007) 14–18.
[33] M. Haruta, CATTECH 6 (2002) 102–115.
[34] J.P. Dacquin, M. Cabié, C.R. Henry, C. Lancelot, C. Dujardin, S.R. Raouf, P. Granger, J. Catal. 270 (2010) 299–309.
[35] M. Chen, D.W. Goodman, Chem. Soc. Rev. 37 (2008) 1860–1870.
[36] C.T. Campbell, S.C. Parker, D.E. Starr, Science 298 (2002) 811–814.
[37] P. Forzatti, L. Lietti, Catal. Today 52 (1999) 165–181.
[38] E. Jang, E.-K. Lim, J. Choi, J. Park, Y.-J. Huh, J.-S. Suh, Y.-M. Huh, S. Haam, Cryst. Growth Des. 12 (2012) 37–39.
[39] M. Di Vece, D. Grandjean, M.J. Van Bael, C.P. Romero, X. Wang, S. Decoster, A. Vantomme, P. Lievens, Phys. Rev. Lett. 100 (2008) 236105.
[40] R.S. Goeke, A.K. Datye, Top. Catal. 46 (2007) 3–9.
[41] S.B. Simonsen, I. Chorkendorff, S. Dahl, M. Skoglundh, J. Sehested, S. Helveg, J. Catal. 281 (2011) 147–155.
[42] S. Bonanni, K. Aït-Mansour, W. Harbich, H. Brune, J. Am. Chem. Soc. 136 (2014) 8702–8707.
[43] Z. Yuan, X.-N. Li, S.-G. He, J. Phys. Chem. Lett. 5 (2014) 1585–1590.
[44] Y.G. Wang, D.H. Mei, V.A. Glezakou, J. Li, R. Rousseau, Nat. Commun. 6 (2015) 8.
[45] F. Yang, M.S. Chen, D.W. Goodman, J. Phys. Chem. C 113 (2009) 254–260.
[46] J. Raskó, J. Kiss, Catal. Lett. 111 (2006) 87–95.
[47] T. Diemant, Z. Zhao, H. Rauscher, J. Bansmann, R.J. Behm, Top. Catal. 44 (2007) 83–93.
[48] K.F. Peters, P. Steadman, H. Isern, J. Alvarez, S. Ferrer, Surf. Sci. 467 (2000) 10–22.
[49] L. Piccolo, D. Loffreda, F.J. Cadete Santos Aires, C. Deranlot, Y. Jugnet, P. Sautet, J.C. Bertolini, Surf. Sci. 566 (2004) 995–1000.
[50] Y. Jugnet, F.J. Cadete Santos Aires, C. Deranlot, L. Piccolo, J.C. Bertolini, Surf. Sci. 521 (2002) L639–L644.
[51] D. Loffreda, L. Piccolo, P. Sautet, Phys. Rev. B 71 (2005) 113414.
[52] J. Hrbek, F.M. Hoffmann, J.B. Park, P. Liu, D. Stacchiola, Y.S. Hoo, S. Ma, A. Nambu, J.A. Rodriguez, M.G. White, J. Am. Chem. Soc. 130 (2008) 17272–17273.
[53] Z. Pászti, O. Hakkel, T. Keszthelyi, A. Berkó, N. Balázs, I. Bakó, L. Guczi, Langmuir 26 (2010) 16312–16324.
[54] J. Wang, M. McEntee, W.J. Tang, M. Neurock, A.P. Baddorf, P. Maksymovych, J.T. Yates, J. Am. Chem. Soc. 138 (2016) 1518–1526.
[55] A. Berkó, F. Solymosi, J. Catal. 183 (1999) 91–101.
[56] P. Wynblatt, N.A. Gjostein, Prog. Solid State Chem. 9 (1975) 21–58.
[57] K.J. Hu, S.R. Plant, P.R. Ellis, C.M. Brown, P.T. Bishop, R.E. Palmer, J. Am. Chem. Soc. 137 (2015) 15161–15168.
[58] M. Valden, X. Lai, D.W. Goodman, Science 281 (1998) 1647–1650.
[59] J.C. Liu, Y.G. Wang, J. Li, J. Am. Chem. Soc. 139 (2017) 6190–6199.
[60] S.C. Parker, C.T. Campbell, Top. Catal. 44 (2007) 3–13.
[61] S.C. Parker, C.T. Campbell, Phys. Rev. B 75 (2007) 035430.
[62] M. Ritter, W. Ranke, W. Weiss, Phys. Rev. B 57 (1998) 7240–7251.
[63] R. Ouyang, W.-X. Li, Phys. Rev. B 84 (2011) 165403.
[64] D.E. Starr, S.K. Shaikhutdinov, H.J. Freund, Top. Catal. 36 (2005) 33–41.
[65] Z.-P. Liu, S. Jenkins, D. King, Phys. Rev. Lett. 93 (2004) 156102.
[66] E. Wahlstrom, N. Lopez, R. Schaub, P. Thostrup, A. Ronnau, C. Africh, E. Laegsgaard, J.K. Norskov, F. Besenbacher, Phys. Rev. Lett. 90 (2003) 026101.
[67] C.F. Sanz-Navarro, P.-O. Åstrand, D. Chen, M. Rønning, A.C.T.v. Duin, J.E. Mueller, W.A. Goddard III, J. Phys. Chem. C 112 (2008) 12663–12668.
[68] R. Ouyang, J.X. Liu, W.X. Li, J. Am. Chem. Soc. 135 (2013) 1760–1771.
[69] K. Poetting, W. Schmickler, T. Jacob, ChemPhysChem 11 (2010) 1395–1404.
[70] C.L. Liu, J.M. Cohen, J.B. Adams, A.F. Voter, Surf. Sci. 253 (1991) 334–344.
[71] R. Gomer, Rep. Prog. Phys. 53 (1990) 917–1002.
[72] R. Ferrando, G. Tréglia, Phys. Rev. Lett. 76 (1996) 2109–2112.
[73] C.N. Singman, J. Chem. Educ. 61 (1984) 137.
[74] L.R. Houk, S.R. Challa, B. Grayson, P. Fanson, A.K. Datye, Langmuir 25 (2009) 11225–11227.
[75] W.R. Tyson, W.A. Miller, Surf. Sci. 62 (1977) 267–276.
[76] J.A. Farmer, C.T. Campbell, Science 329 (2010) 933–936.
[77] S.L. Hemmingson, C.T. Campbell, ACS Nano 11 (2017) 1196–1203.
[78] K. Reuter, M. Scheffler, Phys. Rev. B 65 (2002) 035406.
[79] G. Kresse, J. Furthmuller, Phys. Rev. B 54 (1996) 11169–11186.
[80] P.E. Blöchl, Phys. Rev. B 50 (1994) 17953–17979.
[81] J.P. Perdew, J.A. Chevary, S.H. Vosko, K.A. Jackson, M.R. Pederson, D.J. Singh, C. Fiolhais, Phys. Rev. B 46 (1992) 6671–6687.
[82] G. Henkelman, B.P. Uberuaga, H. Jónsson, J. Chem. Phys. 113 (2000) 9901–9904.
[83] R. Coquet, K.L. Howard, D.J. Willock, Chem. Soc. Rev. 37 (2008) 2046–2076.
[84] S.K. Shaikhutdinov, R. Meyer, M. Naschitzki, M. Baumer, H.J. Freund, Catal. Lett. 86 (2003) 211–219.